Characterization of pediatric head and neck masses with quantitative analysis of diffusion-weighted imaging and measurement of apparent diffusion coefficients

Ali Baiomy[1], Ayman Nada[2,3], Ahmed Gabr[3], Ayda Youssef[3], Esmat Mahmoud[3], Iman Zaky[4]

[1]Texas Tech University Health Sciences Center El Paso, TX, [2]Department of Radiology, University of Missouri, MO, USA, [3]Department of Diagnostic and Interventional Radiology, National Cancer Institute, Cairo University, [4]Department of Radiology, Children's Cancer Hospital, Egypt

Correspondence: Dr. Ayman Nada, Department of Radiology, University of Missouri, USA. E-mail: anada@health.Missouri.edu

Abstract

Purpose: Our objective was to investigate the accuracy of quantitative diffusion-weighted imaging (DWI) to determine the histopathologic diagnosis of pediatric head and neck lesions. **Materials and Methods:** This retrospective study included 100 pediatric patients recently diagnosed with head and neck tumors. All patients underwent preoperative conventional magnetic resonance imaging (MRI) and DWI. Each lesion was evaluated according to signal characteristics, enhancement pattern, and diffusivity. The average apparent diffusion coefficient (ADC) obtained from each tumor was compared to the histological diagnosis of benign, locally malignant, or malignant categories. **Results:** Our retrospective study showed a significant negative correlation between average ADC and tumor histopathologic diagnosis ($P < 0.001$, $r = -0.54$). The mean ADC values of benign, locally malignant lesions, and malignant tumors were $1.65 \pm 0.58 \times 10^{-3}$, $1.43 \pm 0.17 \times 10^{-3}$, and $0.83 \pm 0.23 \times 10^{-3}$ mm^2 s^{-1}, respectively. The ADC values of benign and locally malignant lesions were overlapped. We found a cut-off value of $\leq 1.19 \times 10^{-3}$ mm^{2}s^{-1} to differentiate benign from malignant pediatric head and neck masses with a sensitivity of 97.3%, specificity of 80.0%, positive predictive value of 94.7%, and negative predictive value of 88.9%. **Conclusion:** Diffusion-weighted MRI study is an accurate, fast, noninvasive, and nonenhanced technique that can be used to characterize head and neck lesions. DWI helps to differentiate malignant from benign lesions based on calculated ADC values. Additionally, DWI is helpful to guide biopsy target sites and decrease the rate of unnecessary invasive procedures.

Key words: Apparent diffusion coefficient; DWI; head and neck masses; pediatric

Introduction

Cystic and solid head and neck masses are a common finding in pediatric patients and usually represent a

Access this article online	
Quick Response Code:	Website: www.ijri.org
	DOI: 10.4103/ijri.IJRI_129_19

Cite this article as: Baiomy A, Nada A, Gabr A, Youssef A, Mahmoud E, Zaky I. Characterization of pediatric head and neck masses with quantitative analysis of diffusion-weighted imaging and measurement of apparent diffusion coefficients. Indian J Radiol Imaging 2020;30:473-81.

Received: 17-Mar-2019 **Revised:** 30-Nov-2019
Accepted: 11-Aug-2020 **Published:** 13-Jan-2021

diagnostic dilemma for clinicians and radiologists. It is essential to differentiate benign from malignant pediatric neck tumors as this will inform treatment planning and improve the prognosis of malignant tumors.[1,2]

Different routine magnetic resonance imaging (MRI) pulse sequences can help with soft tissue characterization, yet they cannot accurately differentiate between benign and malignant tumors. Thus, invasive procedures such as biopsies are commonly used, although they may give false results.[2,3]

Diffusion-weighted echo-planar MR imaging is a noninvasive technique that relies on microscopic water motion in tissues. The apparent diffusion coefficient (ADC) represents the extent of translational diffusion of molecules measured in the human body.[4]

Diffusion-weighted imaging (DWI) has been used to differentiate between benign and malignant tumors in different body regions. The clinical importance of DWI and the ADC measurement lies in their ability to provide tissue information at the cellular level.[5]

Diffusion-weighted MR imaging has been recently used for characterization of neck mass in adults.[6] Some researchers found a negative relation between ADC value and the cellularity of the masses,[7,8] while others did not find the ADC value to be a reliable method to differentiate benign from malignant tumors in pediatric patients.[9]

DWI might have an additive role to the conventional MRI in the evaluation of head and neck lesions.[10] The aim of this study was to assess the clinical utility of the calculated ADC value in the characterization of pediatric head and neck masses and differentiation of benign from malignant lesions. We investigated the accuracy of quantitative DWI in determination of the histopathologic diagnosis as well.

Materials and Methods

Patients

We retrospectively reviewed the data for 100 pediatric patients (age range, 4 months–17 years), who presented with head and neck mass during the period from January 2011 to January 2013. Data were obtained from the radiology PACS database.

Inclusions criteria

Patients who had received prior therapy were excluded from the study. Since vascular malformations are the most common, these were also excluded. All diagnoses were histologically confirmed after biopsy or surgical excision.

MRI methods

All patients were evaluated by contrast-enhanced MRI using the Magnetom ESPREE 1.5 T (Siemens, Erlangen, Germany), a 1.5 Tesla super-conducting MR scanner. All MR scans were conducted with patients in the supine position using the following sequences: axial T1 FSE (TR = 450 ms, TE = 12 ms), axial T2 SE (TR = 4540 ms, TE = 96 ms), axial STIR (TR = 9000 ms, TE = 116 ms, TI = 2500 ms), and sagittal T1SE (TR = 430 ms, TE = 10 ms). Other MRI parameters included slice thickness of 5 mm with a 1–2 mm gap and a matrix size of 256 × 256 mm. After intravenous administration of Gadolinium- DTPA (diethylene triamine pentaacetic acid, 0.1 mg/kg), contrast-enhanced T1WI in the axial, sagittal, and coronal planes were obtained.

DWIs were acquired with the following imaging parameters: TR = 3000 ms, TE = 89 ms, slice thickness = 5 mm, interslice gap = 1 mm, FOV = 230 × 180 × 130 mm, matrix = 112 × 70 mm, flip angle = 90°, and EPI factor = 51. DWIs were acquired with b values of 0, 500, and 1000 s/mm^2. Then, ADC maps were automatically regenerated. ADC value was measured by manually placing ROIs of 5–10 mm^2 within tumor regions on the ADC map. We carefully compared the ADC maps and other MR images to place ROIs in central portions of the lesions. We excluded necrotic and hemorrhagic tumor areas. We chose three random ROIs placed as centrally as possible within the tumor area and calculated the average ADC values.

In patients with contrast-enhancing tumors, ROIs were placed on ADC maps at the corresponding site of enhancement that reflects viable tumor tissue. In faintly enhancing or nonenhancing tumors, ROIs were placed after the solid part of the lesion was identified. Necrotic components were diagnosed based on appearance in contrast-enhanced T1-weighted images as nonenhancing regions within enhancing tumors. Hemorrhagic lesions were recognized on nonenhanced T1-weighted MR images as areas of hyperintensity. In the pure cystic lesions, ROIs were placed in the center of the lesions. Two radiologists with 11 and 8 years of experience in head and neck radiology evaluated the MRI exams independently.

Histopathologic classification

The final diagnoses were confirmed at histopathology after an imaging guided biopsy and or open surgical biopsy.

Statistical analysis

Statistical analysis was done using Excel and SPSS (Statistical Package for Social Science version 15). Data were described using the mean and standard deviation. Kolmogorov–Smirnov test was used to check the normality of data distribution before the analysis. Our data were parametric with normal distribution. Student's *t*-test was used to analyze the data for significant differences between two groups, while a one-way ANOVA test was used to compare between more than two groups. The receiver operating curve (ROC) was done to determine the cut-off point with the highest accuracy and sensitivity. The *P* value

was considered statistically significant if ≤0.05 at the 95% confidence interval.

Results

This retrospective study included 100 pediatric patients presented with head and neck masses (64 males and 36 females). Their ages ranged from 4 months to 17 years. Based on histological diagnoses, tumors were subdivided into benign (n = 22 lesions), locally malignant (n = 7 lesions), and malignant masses (n = 71 lesions). The number of benign masses were (n = 22); the most common benign lesion was abscess (n = 3) and neurofibroma (n = 2). Table 1 shows the pathological diagnoses of the benign masses. Rhabdomyosarcoma was the most common malignant pathological diagnosis (n = 26) followed by nasopharyngeal carcinoma (n = 14) and lymphoma (n = 12). Table 2 shows the different pathological diagnosis of the malignant lesions. As shown in Table 3, locally malignant lesions (n = 7) included chordoma (n = 4), primitive myxoid mesenchymal tumor of infancy (n = 2), and one case of giant cell tumor of the bone.

Regarding the location of the masses, the nasopharynx was the most common location (n = 19), followed by the orbit (n = 12), and the masticator space (n = 12).

The mean ADC values of the benign, locally malignant masses, and malignant tumors were 1.65 ± 0.58, 1.43 ± 0.1,7 and 0.83 ± 0.23 × 10^{-3} mm^2 s^{-1}, respectively. Figure 1 shows a box and plot of the ADC values of benign, locally malignant, and malignant pediatric head and neck masses. In general, ADC values of malignant tumors were lower than the values of benign and locally malignant lesions. The ADC values of benign and locally malignant lesions were overlapping. There was a statistically significant difference in ADC values between benign and malignant tumors (P < 0.001), with a strong reverse correlation *(r = -0.54)*. In addition, statistically significant differences in ADC values were also found between locally malignant lesions and malignant tumors (P < 0.001). There was no statistically significant difference in ADC values between benign tumors and locally malignant lesions (P < 0.33).

After exclusion of abscesses, which had a very low ADC value, quantitative analysis revealed that the mean ADC value of benign lesions was 1.65 ± 0.58 × 10^{-3} mm^2 s^{-1}. Benign cystic lesions included cystic hygroma, thyroglossal cyst, coloboma, and epidermoid cyst; the ADC value of these cysts ranged from 1.8 to 3.1 × 10^{-3} mm^2 s^{-1}. Solid lesions included fibromatosis, angiofibroma, hamartoma, teratoma [Figure 2], Warthin tumor, parotid adenoma, inflammatory myofibroblastic tumor (IMT) [Figure 3], and neurofibroma. The ADC value of these lesions ranged from 1.2 to 2.1 × 10^{-3} mm^2 s^{-1}.

The mean ADC value of locally malignant tumors was 1.43 ± 0.17 × 10^{-3} mm^2 s^{-1}. As outlined in Table 2, the mean

Table 1: Frequency and mean ADC value of malignant tumors

Tumor pathology	Frequency	ADC value Mean±STD
Rhabdomyosarcoma	26	0.97±0.19
Nasopharyngeal carcinoma	14	0.82±0.16
Non-Hodgkin's lymphoma	9	0.48±0.10
Metastatic lymph node	5	0.74±0.17
Hodgkin lymphoma	3	0.69±0.03
Neuroblastoma (mets)	3	0.89±0.25
Leukemia	2	0.62±0.01
Atrt	1	3.10
Epithelial carcinoma	1	0.95
Fibrosarcoma	1	1.06
Langerhans cell histiocytosis	1	0.85
Mucoepidermoid carcinoma	1	1.25
Parotid gland undifferentiated carcinoma	1	0.98
Pnet	1	0.64
Retinoblastoma	1	0.88
Undifferentiated carcinoma	1	1.10
Total	71	0.83±0.23

Table 2: Frequency and mean ADC value of locally malignant tumors

Tumor pathology	Frequency	Mean±STD
Chordoma	4	1.43±0.20
Primitive myxoid mesenchymal tumor of infancy (PMMTI)	2	1.50±0.14
Giant cell tumor of bone	1	1.28
Total	7	1.43±0.17

ADC values detected in patients with chordoma and primitive myxoid mesenchymal tumor of infancy [Figure 4] were 1.2 ± 0.17 and 1.4 ± 0.17 × 10^{-3} mm^2s^{-1}, respectively.

The mean ADC value of malignant tumors was 0.83 ± 0.23 × 10^{-3} mm^2 s^{-1}. The mean ADC value of rhabdomyosarcoma 0.97 ± 0.19 × 10^{-3} mm^2 s^{-1} [Figure 5] was similar to that of the nasopharyngeal carcinoma 0.82 ± 0.16 × 10^{-3} mm^2 s^{-1} [Figure 6], whereas lymphoma showed the lowest ADC value 0.34 ± 0.08 × 10^{-3} mm^2 s^{-1}. The atypical teratoid rhabdoid tumor, an aggressive malignant tumor, had an ADC value of 0.66 × 10^{-3} mm^2 s^{-1}. Table 2 shows the mean ADC value of all malignant lesions in the study cohort.

DWI was useful in differentiating between pyogenic abscess and necrotic malignant lesions as well as benign cysts. The cystic component of abscesses showed restricted diffusivity as it contained viscous pus with decreased water molecule motion. In contrast, necrotic malignant lesions showed facilitated diffusivity [Figure 7].

The ROC curve [Figure 8] showed that the ADC cut-off value for differentiating between benign and malignant pediatric head and neck masses was ≤1.19 × 10^{-3} mm^2 s^{-1}

Table 3: Frequency and mean ADC value of benign lesions after exclusion of the three cases of abscesses

Tumor pathology	Frequency	Mean ADC
Fibromatosis	2	1.23
Neurofibroma	2	1.99
Angiofibroma	1	1.5
Coloboma	1	2.66
Cystic hygroma	1	3.10
Epidermoid cyst	1	2.60
Fibrous dysplasia	1	1.50
Hamartoma	1	1.30
Hemangioma	1	1.10
IMT	1	1.6
Parotid inflammation (sialadenitis)	1	1.06
Lymphadenitis necrotic (TB)	1	1.71
Optic nerve glioma	1	1.08
Parapharyngeal teratoma	1	1.31
Parotid gland adenoma	1	2.23
Plexiform NF	1	1.30
Thyroglossal cyst	1	1.40
Warthin tumor	1	2.36
Total	19	1.65

with a sensitivity of 97.3%, specificity of 80.0%, positive predictive value of 94.7%, and negative predictive value of 88.9%. The ROC curve showed that the threshold ADC value for differentiation between locally malignant masses and malignant tumors was ≤1.19 × 10^{-3} mm^2 s^{-1} with a sensitivity of 97.3%, specificity of 100.0%, positive predictive value of 100.0%, and negative predictive value of 77.8%. The ADC value of locally malignant tumors overlapped that of the benign masses.

Discussion

Head and neck tumors warrant special knowledge of their prevalence and typical imaging features.[11] Differentiation of malignant tumors from benign lesions is crucial as many malignant conditions have an excellent prognosis with early and appropriate management.[12] Thus, imaging has an important role in the characterization and assessment of the extent of head and neck lesions.[11]

To evaluate head and neck masses, conventional MRI and CT still are the primary imaging modalities, despite their low sensitivity and accuracy.[12] Moreover, post-treatment changes can be difficult to differentiate from tumor recurrence, as both entities may present with similar imaging features.[10,12]

DWI is an adjunct tool that could help tumor detection, tumor characterization, differentiation of tumor tissue from nontumor tissue, and prediction and monitoring of treatment response.[11] DWI has been proposed as a sensitive marker for monitoring treatment response in head and neck cancer.[13]

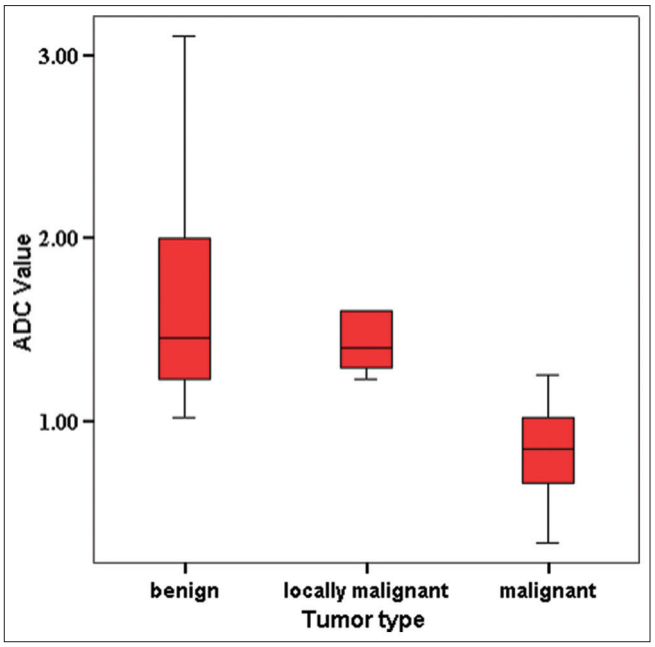

Figure 1: Box and whisker plot of pediatric head and neck masses. Malignant tumors show lower ADC values than benign masses

In this retrospective study, after analyzing 100 cases, the mean ADC value of malignant pediatric head and neck tumors was significantly lower than that of benign lesions. Rhabdomyosarcoma was the most common malignant tumor in our cohort. This was found to be discordant with the international consensus that lymphoma is the most common pediatric malignant head and neck tumor.[2,3] However, this might be explained by our relatively small cohort or different epidemiology in our region. Thus, further studies on a larger cohort are required to revalidate the epidemiology of pediatric head and neck tumors in Indian children. Due to the predominance of nasopharyngeal masses as well as the involvement of the nasopharynx in cases of rhabdomyosarcoma, the nasopharynx was the most common location of malignant tumors.

The mean ADC values in our study were as follows: the ADC values of malignant lesions were found to be lower than those of benign lesions, while the ADC values of locally malignant lesions overlapped with those of benign lesions. Table 4 shows the results of prior studies regarding mean ADC values.

The results of this study demonstrated that cystic hygroma had the highest ADC value among benign tumors 3.1 ± 0.08 × 10^{-3} mm^2 s^{-1}. Wang *et al.*, 2001 reported that the mean ADC value of benign cystic lesion in adult head and neck is 2.05 ± 0.62 × 10^{-3} mm^2 s^{-1}. They also reported that the difference in ADC values among cystic lesions might be due to varying protein concentrations of the lesions.[14]

Among benign solid tumors, parapharyngeal teratoma showed a high ADC, at 2.3 ± 0.01 × 10^{-3} mm^2s^{-1}. IMT is a rare

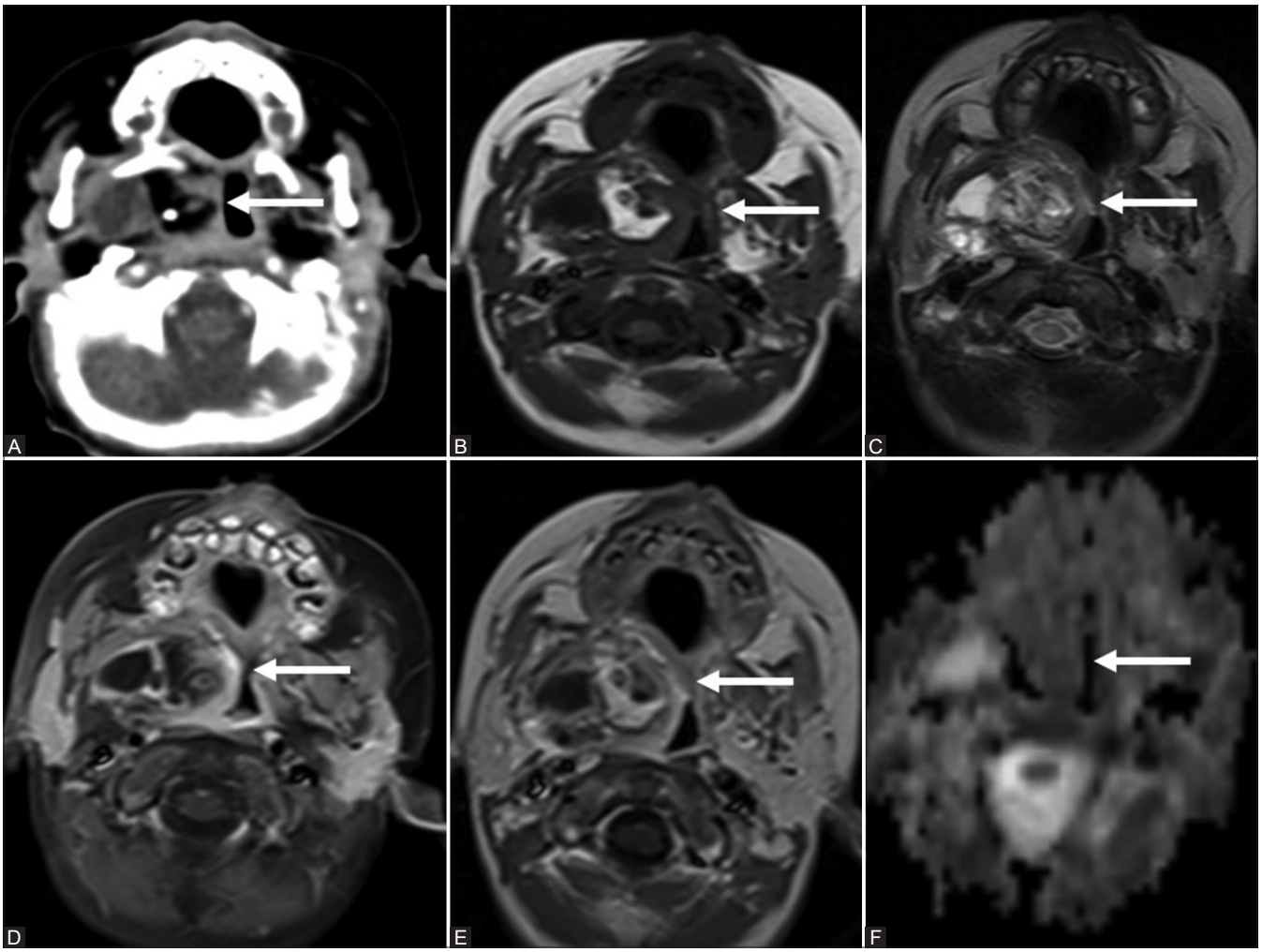

Figure 2 (A-F): Mature teratoma in a 1.5-year-old female patient presented with right check fullness. Axial contrast-enhanced CT- (A), axial T1- (B), and T2- (C) weighted images show well-circumscribed right parapharyngeal mass with internal soft tissue, fluid, fat, and calcifications (arrows). Axial fat (D) and nonfat saturated (E) postcontrast images show heterogeneous enhancement with characteristic signal drop of its fat component (arrows). Axial ADC map (F) shows heterogeneous signal with calculated ADC (2.2 x 10^{-3} mm^2/s)

Table 4: Comparison of mean ADC values of prior studies

The study	No of pts.	Mean ADC value Ave. ± SD ($\times 10^{-3} mm^2 s^{-1}$)		
		Malignant tumors	Benign solid tumors	Benign cystic lesions
Wang *et al*. 2001[14]	97 pts	1.22±0.43	1.56±0.51	2.05±0.62
Sumi *et al*. 2006[15]	26 pts	1.167±0.447 for metastatic LNs 0.601±0.427 for lymphoma	0.652±0.101 for benign LNs	
Maeda 2007[16]	39 pts with SCC 14 pts with lymphoma	0.96±0.11 for SCC 0.65±0.09 for lymphoma		
Sakamoto 2009[17]	67 pts	1.23±0.45	1.48±0.62	2.41±0.48
AbdelRazek, 2009[18]	78 pts	0.93±0.18	1.57±0.26	2.01±0.21
ElShahat *et al*., 2013[19]	43 pts	1.02±0.22	1.62±0.27	
Serifoglu *et al*. 2015[20]	90 pts	0.72 for malignant 0.44 for lymphoma 0.72 for SCC	1.17	
Ertem, 2016[21]	102 pts	1.27±0.57	1.61±0.67	
Kanmaz, 2018[22]	32 pts	0.90±0.17	1.57±0.42	

benign neoplasm of mesenchymal origin with unknown etiology, which occurs primarily in soft tissue and in numerous anatomic locations. IMT has been reported mainly in children and young adults. Because of the rarity of IMT and the fact that the lesions often mimic sarcoma, lymphoma, and metastasis, IMT can often be clinically misdiagnosed as a malignant tumor. We found a case of maxillary IMT misdiagnosed as rhabdomyosarcoma based on the

conventional MRI criteria. The ADC value of such a lesion was 1.6×10^{-3} mm^2 s^{-1}. This is another example, in addition to the primitive myxoid mesenchymal tumor of infancy, of the usefulness of DWI in reducing the rate of false negative cases.

Locally malignant tumors have an aggressive appearance in conventional MRI images and overlapping ADC values with benign solid tumors. Our two cases of primitive myxoid mesenchymal tumor of infancy [Figure 6] were a good example of the usefulness of DWI in the characterization of such lesions. Myxoid mesenchymal tumor of infancy [Figure 6] is a recently recognized soft tissue tumor with only few reported cases.

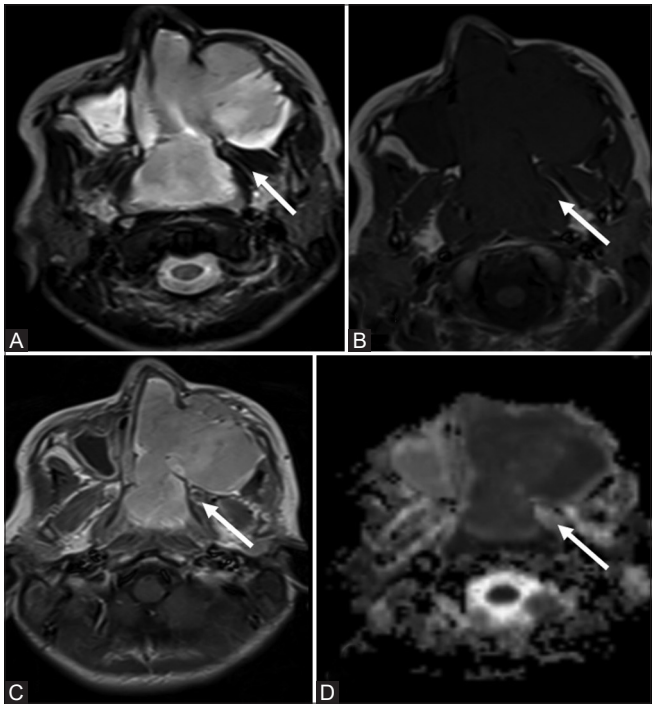

Figure 3 (A-D): Sinonasal inflammatory myofibroblastic tumor in a 13-year-old female patient presenting with chronic headache and left cheek fullness**.** Axial T2- (A) and T1- (B) weighted images show extensive left maxillary sinus mass (white arrows) of T1 hypo intense signal and T2 hyper intense signal with significant extension into the left nasal cavity and nasopharynx. Axial T1 postcontrast image (C) shows diffuse enhancement of the mass (arrow). Axial ADC map (D) reveals dark signal of the mass, indicative of restricted diffusivity with ADC value (1.06 x 10 $^{-3}$ mm²/s)

The lower ADC value of the malignant lesions is attributed to differences in histopathologic features between benign and malignant tumors. Malignant tumors show hypercellularity with enlarged nuclei, hyperchromatism, and angulation of nuclear contour. Such histological characteristics reduce the extracellular matrix and the diffusion space of water protons in the extracellular and intracellular dimensions with a resultant decrease in ADCs.[14]

Sumi *et al*., 2006 reported that the mean ADC value of lymphomas is lower than that of metastatic lymph nodes due to differences in cellularity.[15] Maeda *et al*., 2007 and Sumi *et al*., 2006 added that squamous cell carcinoma has a higher ADC value than lymphoma because carcinoma may contain small foci of necrosis on histopathological examination that are not identifiable on MR images.[15,16]

DWI also differentiated pyogenic abscess from necrotic components of malignant tumors.[13] Necrotic malignant cervical lymph nodes show facilitated diffusion in contrast to the inflammatory pyogenic or granulomatous lymph nodes, which show restricted diffusion due to thick pus in the pyogenic and caseous material in granulomatous nodes [Figure 7]. The central cystic component of abscesses showed restricted diffusivity as it contained viscous pus with decreased water molecule motion. In contrast, the necrotic components of malignant nodes showed facilitated diffusivity.[13]

Owing to its speed and lower motion artifact, diffusion-weighted MR imaging using echo-planar imaging provides reliable

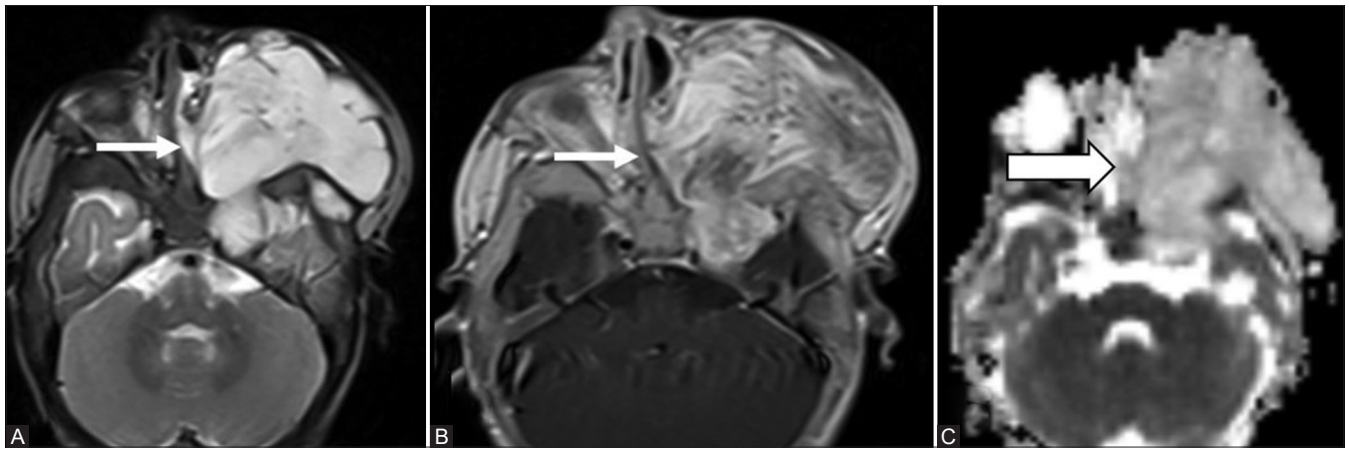

Figure 4 (A-C): Primitive myxoid mesenchymal tumor of the infancy in a 5-month-old girl presenting with large cheek mass. Axial T2-weighted image (A) shows marked T2 hyperintense signal of large left maxillary mass lesion extending into the right orbit and through the optic canal to the intracranial cavity (arrow). Axial T1 postcontrast image (B) demonstrates the heterogeneous intense enhancement of the mass (arrow). Axial ADC map (C) shows hyperintense signal of the mass (outlined arrow) with calculated ADC value (1.66×10^{-3} mm^2/s)

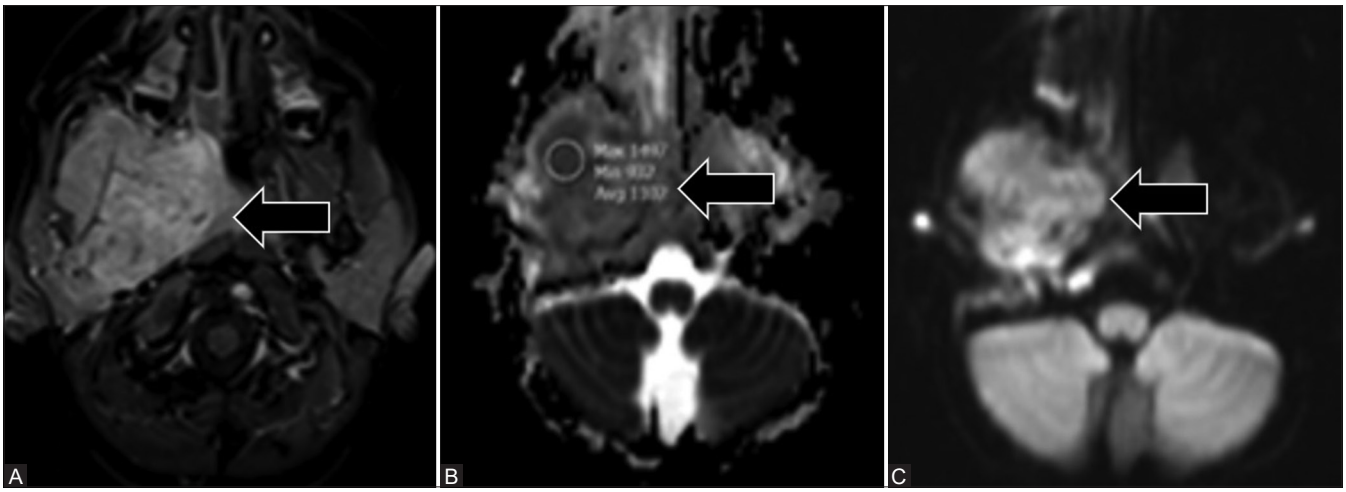

Figure 5 (A-C): Right masticator space rhabdomyosarcoma in a 6-year-old female. Axial T1 postcontrast with fat saturation image (A) demonstrates large infiltrative heterogeneously enhancing soft tissue mass lesion centered upon the right masticator space (arrow) and invading the surrounding structures. Axial ADC map (B) and diffusion-weighted image (C) demonstrate marked restricted diffusivity of the mass (arrows) with low ADC value ($1.02 \times 10^{-3} mm^2/s$)

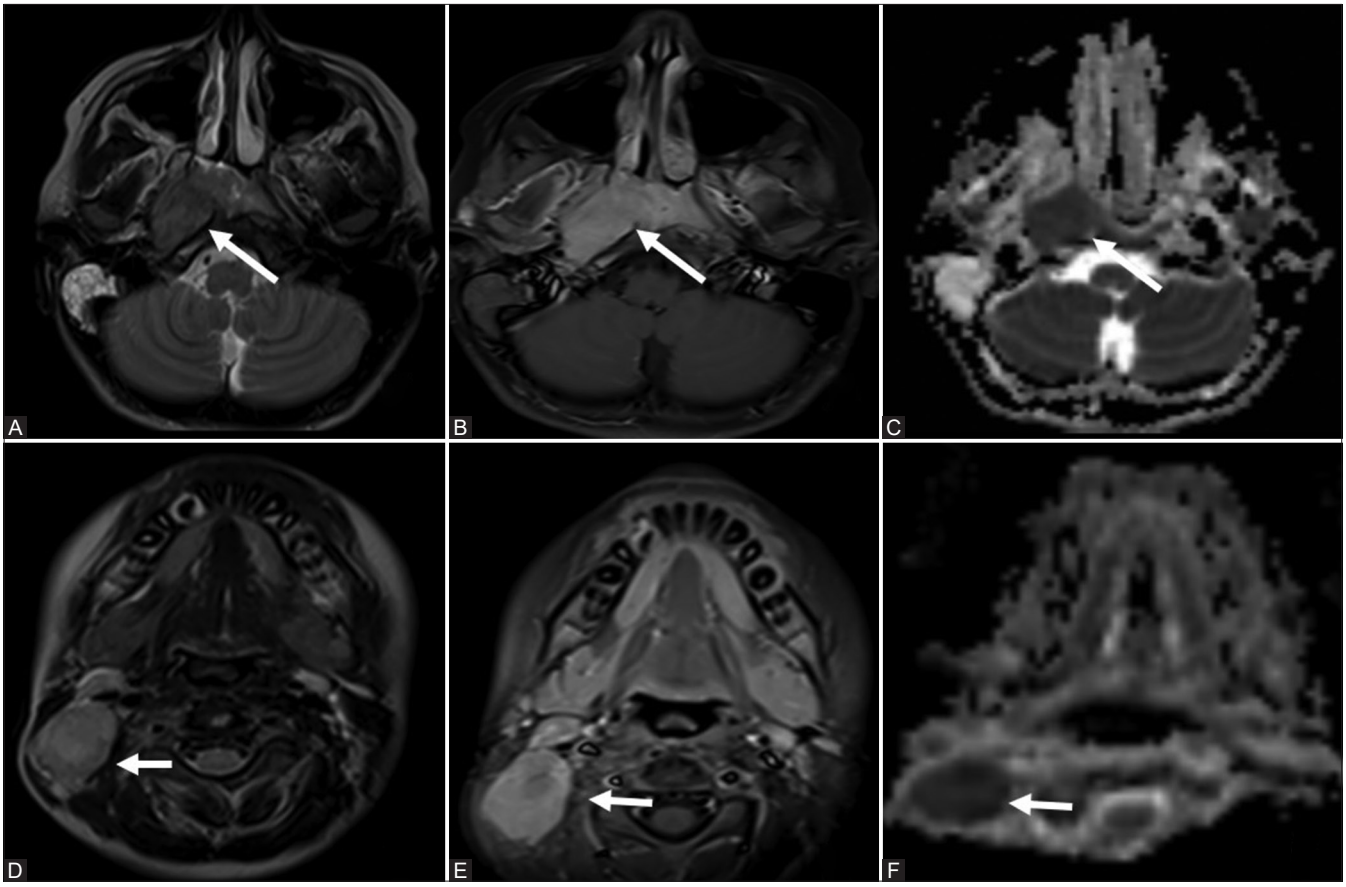

Figure 6 (A-F): Undifferentiated nasopharyngeal carcinoma in a 10-year-old male patient presenting with right cervical mass lesion**.** Axial T2-weighted image (A), T1 contrast-enhanced image with fat saturation (B) and ADC map (C) show large nasopharyngeal mass (arrows) with iso-hypo intense T2 signal and uniform enhancement. The calculated ADC value was ($0.85 \times 10^{-3} mm^2/s$). Axial T2-weighted image (D), T1 contrast-enhanced image with fat saturation (E), and ADC map (F) at a lower level demonstrate associated enlarged right level 2b cervical lymph nodes (short arrows). The calculated ADC value of lymphadenopathy was ($0.95 \times 10^{-3} mm^2/s$)

results in pediatric patients.[23] Diffusion-weighted echo-planar pulse sequence is the sequence of choice for the quantitative study of diffusion as the diffusion and relaxation effects contribute separately to the MR signal intensity and can be easily separated.[24] Furthermore, EPI is a very fast technique that enables data acquisition, with different b values within a

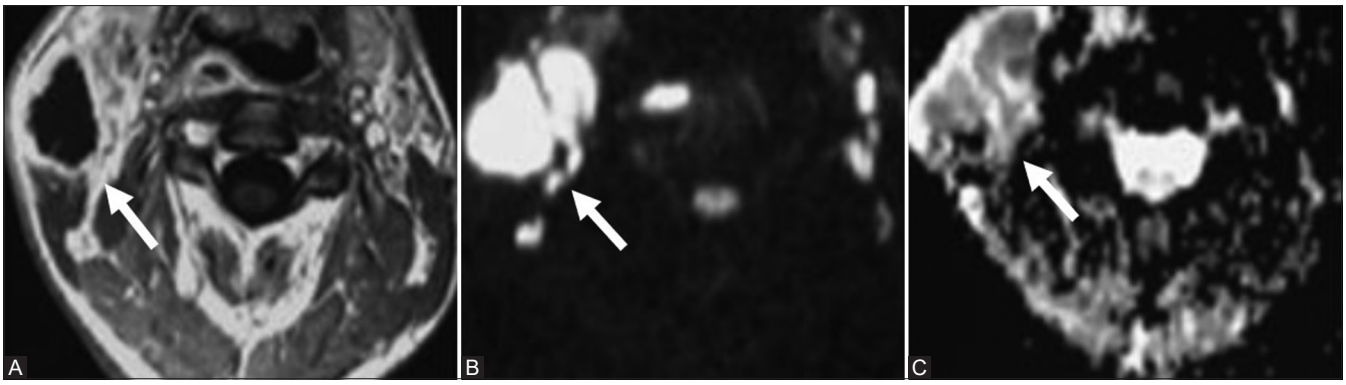

Figure 7 (A-C): Right submandibular abscess 11-year-old female patient presenting with right submandibular mass. Axial T1 postcontrast image (A) shows well-defined irregular peripherally enhancing fluid collection (arrow) within the right submandibular space. Axial diffusion-weighted image (B) and ADC maps (C) demonstrate significant restricted diffusivity of the core of the collection (arrows) with calculated ADC value (0.36×10^{-3} mm^2/s)

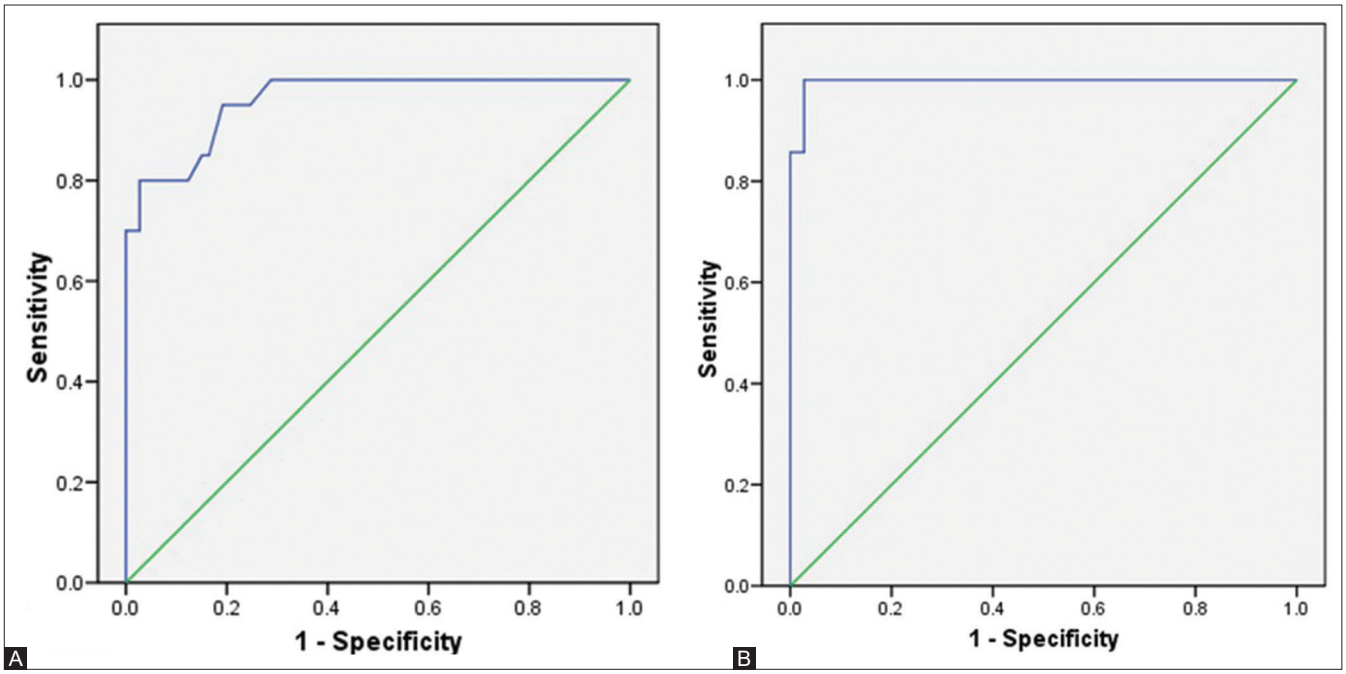

Figure 8 (A and B): (A) Receiver operating characteristic (ROC) curve of the ADC value used for differentiating malignant tumors from benign lesions (B) Receiver operating characteristic (ROC) curve of the ADC value used for differentiating malignant tumors from locally malignant lesions

reasonably short time.[19] The main trade-off of the EPI pulse sequence is that it is very sensitive to magnetic susceptibility effects, resulting in geometric distortion artifacts that tend to be more severe with increasing b values.[23] On the other hand, spin echo can be used for head and neck, although it has less susceptibility to artifacts; it requires a longer acquisition time.[24]

There are some limitations in this study. First, the group of patients was heterogeneous with different pathological entities and different age groups of infants and children. Second, the number of benign tumors was relatively small compared to the number of malignant lesions. Future studies on larger cohorts may further support our hypothesis of the value of diffusion-weighted MR imaging in pediatric tumors. Third, the tumors in our study had originated from different compartments of the head and neck. Further studies could focus on tumors in specific and separate compartments such as orbit, nasopharynx, parotid, and cervical lymph nodes.

Conclusion

Diffusion-weighted MR imaging is a rapid noninvasive and accurate imaging tool for the characterization of pediatric head and neck masses as it can help differentiate malignant from benign lesions. Therefore, we recommend including DWI to routine MR imaging of pediatric head and neck masses.

Financial support and sponsorship

This research received no specific grant from any funding agency in the public, commercial or not-for-profit sectors.

Conflicts of interest

There are no conflicts of interest.

References

1. Brown RE, Harave S. Diagnostic imaging of benign and malignant neck masses in children: A pictorial review. Quant Imaging Med Surg 2016;6:591-604.
2. Cesmebasi A, Gabriel A, Niku D, Bukala K, Donnelly J, Fields PJ, *et al*. Pediatric head and neck tumors: An intra-demographic analysis using the SEER* database. Med Sci Monit 2014;20:2536-42.
3. Sengupta S, Pal R, Saha S, Bera SP, Pal I, Tuli IP. Spectrum of head and neck cancer in children. J Indian Assoc Pediatr Surg 2009;14:200-3.
4. Meuwly JY, Lepori D, Theumann N, Schnyder P, Etechami G, Hohlfeld J, *et al*. Multimodality imaging evaluation of the pediatric neck: Techniques and spectrum of findings. Radio Graphics 2005;25:931-48.
5. Thoeny H, Keyzer F. Extracranial applications of diffusion-weighted magnetic resonance imaging. Eur Radiol 2007;17:1385-93.
6. Lee EJ, terBrugge K, Mikulis D, Choi DS, Bae JM, Lee SK, *et al*. Diagnostic value of peritumoral minimum apparent diffusion coefficient for differentiation of glioblastoma multiforme from solitary metastatic lesions. AJR Am J Roentgenol 2011;196:71-6.
7. Thoeny HC. Diffusion-weighted MRI in head and neck radiology: Applications in oncology. Cancer Imaging 2011;10:209-14.
8. Bhatt N, Gupta N, Soni N, Hooda K, Sapire JM, Kumar Y. Role of diffusion-weighted imaging in head and neck lesions: Pictorial review. Neuroradiol J 2017;30:356-69.
9. Olsen OE, Sebire NJ. Apparent diffusion coefficient maps of pediatric mass lesions with free-breathing diffusion-weighted magnetic resonance: Feasibility study. Acta Radiol 2007;47:198-204.
10. Humphries PD, Sebire NJ, Siegel MJ, Olsen OE. Tumors in pediatric patients at diffusion-weighted MR imaging: Apparent diffusion coefficient and tumor cellularity. Radiology 2007;245:848-54.
11. Koontz NA, Wiggins RH 3rd. Differentiation of benign and malignant head and neck lesions with diffusion tensor imaging and DWI. Am J Roentgenol 2017;208:1110-5.
12. Dickson PV, Davidoff AM. Malignant neoplasms of the head and neck. Semin Pediatr Surg 2006;15:92-8.
13. Stern JS, Ginat DT, Nicholas J, Ryan ME. Imaging of pediatric head and neck masses. Otolaryngol Clin North Am 2015;48:225-46.
14. Wang J, Takashima S, Takayama F, Kawakami S, Saito A, Matsushita T, *et al*. Head and neck lesions: Characterization with diffusion weighted echo-planar MR imaging. Radiology 2001;220:621-30.
15. Sumi M, Van Cautern M, Nakamura T. MR microimaging of benign and malignant nodes in the neck. AJR Am J Roentgenol 2006;186:749-57.
16. Maeda M, Kato H, Sakuma H, Maier SE, Takeda K. Usefulness of the apparent diffusion coefficient inline scan diffusion weighted imaging for distinguishing between squamous cell carcinomas and malignant lymphomas of the head and neck. AJNR Am J Neuroradiol 2007;26:1186-92.
17. Sakamoto J, Yoshino N, Okochi K, Imaizumi A, Tetsumura A, Kurohara K, *et al*. Tissue characterization of head and neck lesions using diffusion-weighted MR imaging. Eur J Radiol 2009;69:260-8.
18. Abdel Razek AA, Gaballa G, Elhawarey G, Megahed AS, Hafez M, Nada N. Characterization of pediatric head and neck masses with diffusion-weighted MR imaging. Eur Radiol 2009;19:201-8.
19. El Shahat HM, Fahmy HS, Gouhar GK. Characterization of head and neck lesions with diffusion-weighted MR imaging and the apparent diffusion coefficient values. Egypt J Radiol Nucl Med 2013;44:791-8.
20. Şerifoğlu İ, Oz İİ, Damar M, Tokgöz Ö, Yazgan Ö, Erdem Z. Diffusion-weighted imaging in the head and neck region: Usefulness of apparent diffusion coefficient values for characterization of lesions. Diagn Interv Radiol 2015;21:208-14.
21. Ertem Åž, Toru HS, Derin AT, Karaali K. Contribution of diffusion-weighted MR images in the differentiation of benign and malign head and neck mass lesions. J Cancer Prev Curr Res 2016;4:00126. doi: 10.15406/jcpcr. 2016.04.00126.
22. Kanmaz L, Karavas E. The role of diffusion-weighted magnetic resonance imaging in the differentiation of head and neck masses. J Clin Med 2018;7:130.
23. Suh CH, Choi YJ, Baek JH, Lee JH. The diagnostic value of diffusion-weighted imaging in differentiating metastatic lymph nodes of head and neck squamous cell carcinoma: A systematic review and meta-analysis. AJNR Am J Neuroradiol 2018;39:1889-95.
24. Thoeny HC, De Keyzer F, King AD. Diffusion-weighted MR imaging in the head and neck. Radiology 2012;263:19-32.